Available online at www.sciencedirect.com

SCIENCE DIRECT®

Global and Planetary Change 41 (2004) 135–145

GLOBAL AND PLANETARY CHANGE

www.elsevier.com/locate/gloplacha

Late Miocene–Pliocene development of Asian aridification as recorded in the Red-Earth Formation in northern China

Zhengtang Guo[a,b,*], Shuzhen Peng[a,c], Qingzhen Hao[a], Pierre E. Biscaye[d], Zhisheng An[b], Tungsheng Liu[a]

[a] *Institute of Geology and Geophysics, Chinese Academy of Sciences, P.O. Box 9825, Beijing 100029, China*
[b] *SKLLQG, Institute of Earth Environment, Chinese Academy of Sciences, P.O. Box 17, Xian 710054, China*
[c] *Tai'an Teacher's College, Tai'an 271000, China*
[d] *Lamont-Doherty Earth Observatory of Columbia University, PO Box 1000, Palisades, NY 10964-8000, USA*

Abstract

In northern China, the Late Miocene–Pliocene *Hipparion Red-Earth Formation* in the eastern Loess Plateau fills a gap of climate records between the well-known loess-soil sequences of the last 2.6 Ma and the Miocene loess-soil sequences from the western Loess Plateau. Earlier studies on type sections indicate that a major part of the Red-Earth Formation is also of wind-blown origin, covering the period from ~7–8 to ~2.6 Ma BP. Because the eolian dust deposited in the region originated from the Asian desert lands, the Red-Earth must contain a record of the aridification history of the Asian interior. In this study, the Xifeng type section in the eastern Loess Plateau is studied to assess the development of Asian aridification during Late Miocene–Pliocene time. Eolian dust deposition continued at the central Loess Plateau since ~6.2 Ma BP, indicating that sizable desert lands in the interior of Asia and the Asian winter monsoon must have been constantly maintained during Late Miocene–Pliocene time, and were able to provide a significant amount of eolian dust. The aridity in the source areas was stronger from ~6.2 to ~5 Ma BP and weaker from ~5 to ~3.6 Ma BP. Two major aridification steps are observed at ~3.6 and ~2.6 Ma BP, respectively. The intensification of eolian deposition at ~3.6 Ma BP is synchronous with a suggested uplift of portions of the Tibetan Plateau. The general aridification history is also highly consistent with the ongoing high-latitude cooling and the consequent expansion of Arctic sea-ice/ice sheets during this interval. Our results therefore suggest that both Tibetan uplift and ice-building processes in the northern hemisphere were two prominent driving forces behind the long-term desertification in the interior of Asia during Late Miocene and Pliocene time.

Keywords: East Asian aridification; Miocene–Pliocene eolian deposition; Winter monsoon; *Hipparion* Red-Earth Formation

1. Introduction

In the eastern Loess Plateau in northern China, the well-known loess-soil sequences of the last 2.6 Ma (Liu, 1985; Kukla, 1987) are underlain in several sedimentary basins by the so-called *Hipparion Red-Earth Formation*, also referred to as *Red Clay deposits* (Liu, 1985). This formation fills a gap of

* Corresponding author. Institute of Geology and Geophysics, Chinese Academy of Sciences, P.O. Box 9825, Beijing 100029, China. Tel.: +86-10-62008110; fax: +86-10-62032495.
E-mail addresses: ztguo@95777.com, ztguo@mail.igcas.ac.cn (Z. Guo).

0921-8181/$ - see front matter © 2004 Elsevier B.V. All rights reserved.
doi:10.1016/j.gloplacha.2004.01.002

the climate records in northern China between the well-known loess-soil sequences of the last 2.6 Ma and the Miocene loess-soil sequences recently reported from the western Loess Plateau (Guo et al., 2002). Magnetostratigraphic studies (Zheng et al., 1992; Yue, 1995; Ding et al., 1998; Sun et al., 1998a,b; Qiang et al., 2001) suggest that the complete sequence of the Red-Earth extends back to ~6–8 Ma BP without significant hiatus, and therefore contains a near continuous record of the late Miocene–Pliocene paleoclimate. The most complete Red-Earth sequences, as we shall refer to them, are usually preserved in sedimentary basins in the eastern Loess Plateau, known as the *Yuan,* or basin areas (Liu, 1985). The thickness of the Red-Earth sequence varies from 50 to 60 m at most of the localities (Zheng et al., 1992; Yue, 1995; Sun et al., 1998a; Qiang et al., 2001). Recently, a number of Red-Earth sequences have been studied, confirming their eolian origin (Ding et al., 1998; Guo et al., 2001). Eolian dust deposition therefore continued in northern China from ~22 Ma BP (Guo et al., 2002) to the present-day (Liu, 1985).

The wind-blown loess-soil sequence in the region studied has provided much information on the evolution of the Asian dry lands and on paleo-atmospheric circulation (e.g. Liu, 1985; An and Porter, 1997; Guo et al., 1998, 2000, 2002). It has been confirmed that the eolian dust deposition of the loess-soil sequence in the middle reaches of the Yellow River mainly originated from the desert lands in northern and northwestern China through the transportation by northwesterly winter monsoon winds (Liu, 1985; An and Porter, 1997; Guo et al., 2002). The existence of dry lands in Asia and a seasonal dust-carrying atmospheric circulation are thus two necessary conditions for eolian dust deposition in the Loess Plateau region. Consequently, the Red-Earth eolian sequence must have documented the history of the desert lands in Asia and the related atmospheric circulation for Late Miocene–Pliocene time.

Based on the studies of the Red-Earth sequence at Xifeng (Fig. 1), a type section of the Red-Earth sequences in the eastern Loess Plateau region, the objective of this paper is to address the Late Miocene–Pliocene history of the aridification in Asia and its primary driving forces.

1.1. General setting and methods

The Xifeng (Fig. 1) basin (also referred to as the Dongzhi *Yuan*) is one of the largest Cenozoic sedimentary basins in the central Loess Plateau region, where the loess-soil sequence of the last 2.6 Ma has been the object of numerous studies (e.g. Kukla, 1987; Kukla and An, 1989; Guo et al., 1991, 2000). Magnetostratigraphic measurements (Sun et al., 1998a) have dated the lower boundary of the Red-Earth at ~7.6 Ma BP. The contact with the overlying loess-soil sequence is near the Matuyama/Gauss magnetic boundary, i.e. ~2.6 Ma. The fact that this sequence records the major magneto-stratigraphic units from ~7.6 to ~2.6 Ma BP indicates that it contains a near continuous record of paleoclimate.

Recently, the section was systematically studied using macro- and micro-morphological, sedimentological, major- and trace-elemental analyses (Guo et al., 2001) in order to characterize the origin of the Red-Earth sequence. The results showed that the lower section older than 6.2 Ma BP is a water-reworked deposit (Fig. 2) due to alluvial and slope processes, while the upper part of the section is of eolian origin, as is demonstrated by its high similarity to typical eolian loess, e.g. mineral composition, grain morphology, sedimentological parameters and geochemical properties (Guo et al., 2001).

In this study, only the eolian part of the section was analyzed. The depth–age relationship was determined based on the magnetostratigraphic results of Sun et al. (1998a). Five hundred and sixty dry bulk samples were taken at 10-cm intervals for mass magnetic susceptibility measurements that were performed on a Bartington magnetic susceptibility meter. In order to address the changes of eolian grain-size geochemically, major elemental abundances of 90 samples were analyzed by X-Ray fluorescence with analytical uncertainties of ±2% for all the major elements except for P_2O_5 and MnO (up to ±10%). The grain-size distribution of 180 bulk samples was also determined using a SALD-3001 laser diffraction particle analyzer. Ultrasonic dispersion, aided by the addition of 20% $(NaPO_3)_6$ solution, was used for grain-size measurement with a precision of about ±3.5%.

In continental eolian records, the materials are usually affected by syn- and post-depositional weathering and pedogenesis during warm and humid peri-

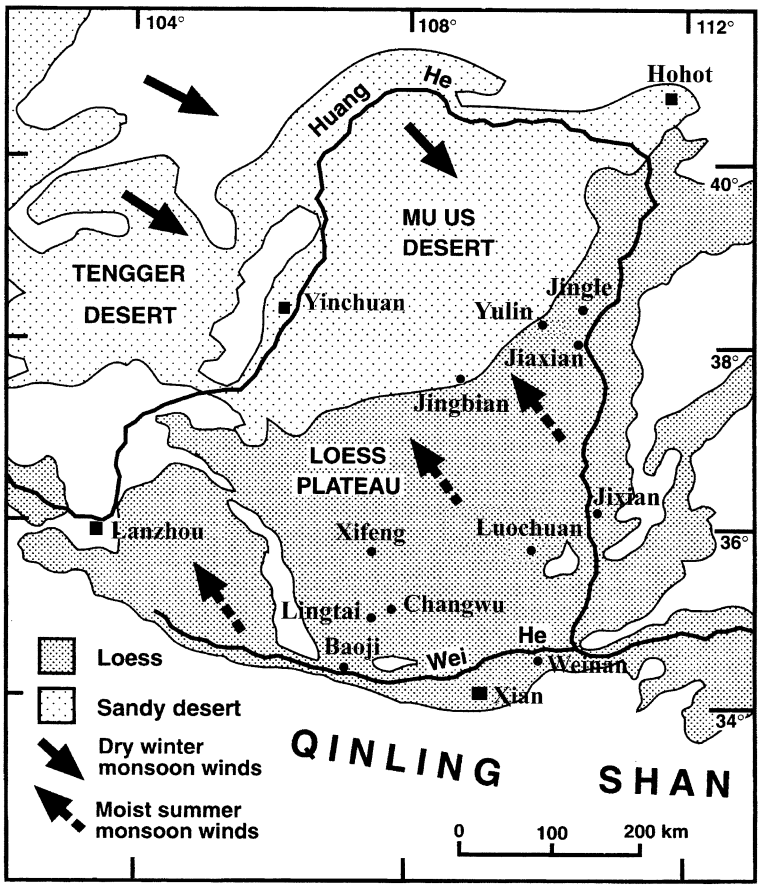

Fig. 1. Map showing the Loess Plateau in northern China, the locations of the sites mentioned in the text, and the modern East-Asian summer and winter monsoon circulations (modified after An and Porter, 1997).

ods (Guo et al., 1996, 2000). This may lead to substantial changes in the grain-size distribution of the original eolian material. Thus, the grain-size data obtained by direct grain-size analyses reflect a mixed effect of depositional and post-depositional processes. For this reason, we attempted to explore a geochemical indicator of eolian dust. Two typical loess samples, respectively, from Xifeng (XF-L1-21) and Jixian (JX-L1-608), and two weakly weathered Red-Earth samples from Xifeng (XF-RE-107 and XF-RE-211) were selected for this purpose (Fig. 3). The samples were separated into 14 size fractions (<1, 1–2, 2–3.9, 3.9–5, 5–10, 10–15.6, 16.6–22.1, 22.1–31.2, 31.2–50, 50–76, 76–88, 88–105, 105–125 and >125 μm) using the classical sedimentation method according to Stoke's Law. Each fraction was then analyzed by X-Ray fluorescence using a Philips PW-1400 unit to determine the major-element abundances. We assume that these four samples, especially the two typical loess samples, have not been significantly weathered, and that the measured grain size represents that of the eolian dust prior to the post-depositional processes. Microscopic observations confirm that the two loess samples still contain more than 10% of detrital carbonate, indicating the weakness of weathering.

To verify the relationship between the geochemical properties and the measured grain size of bulk loess samples, the chemical composition and grain size of 38 Quaternary loess samples from Xifeng (Fig. 3) were analyzed by X-Ray fluorescence and laser diffraction particle-analyzing methods as described above.

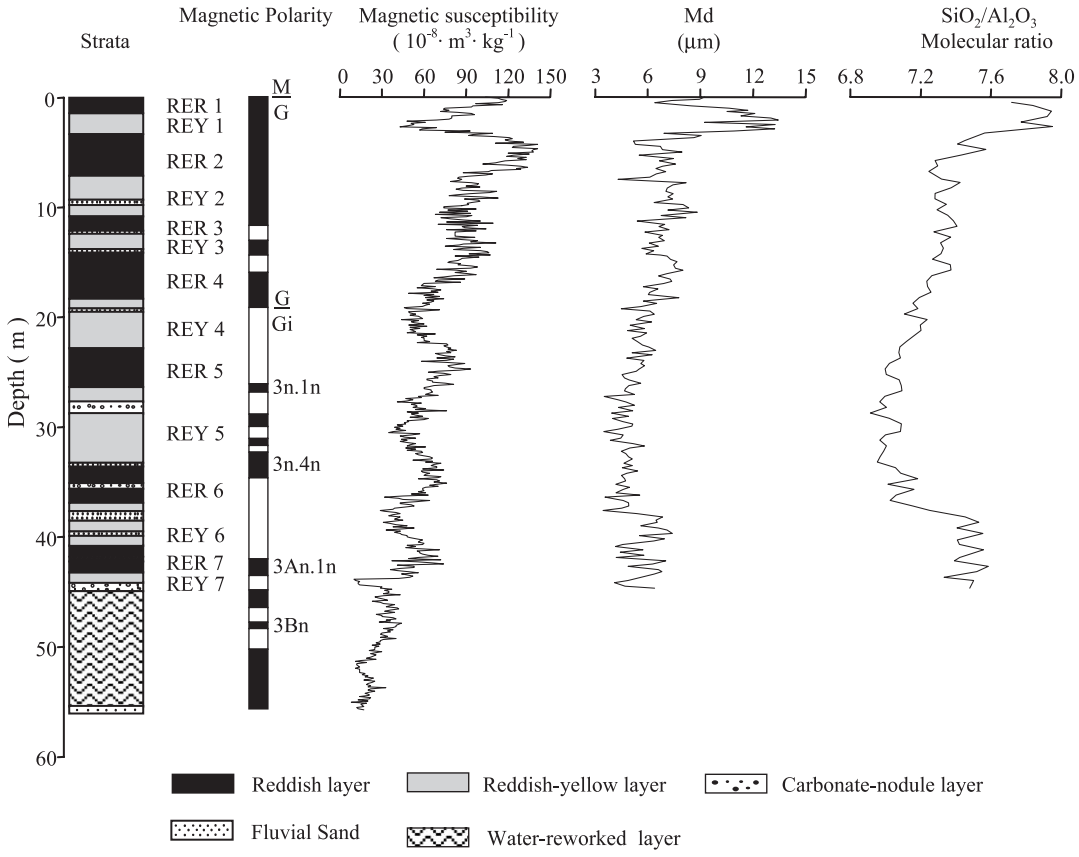

Fig. 2. Lithostratigraphic sequence, magnetic polarity, variations of mass magnetic susceptibility, median grain size (Md) and the SiO_2/Al_2O_3 molecular ratio of the Xifeng Red-Earth sequence. Data for magnetic polarity is from Sun et al. (1998a).

1.2. Intensity of eolian deposition in northern China

In both terrestrial and marine records, the intensity of eolian deposition is usually characterized by dust accumulation rate. This parameter mainly reflects the aridity in the source areas (Hovan et al., 1989; Rea et al., 1998) because stronger aridity leads to enlargement of source areas, to deflation of more dust, and thus to the increase in eolian accumulation rate.

The linear accumulation rate (LAR) of the Xifeng Red-Earth section is given in Fig. 2 (versus depth) and Fig. 4 (versus age) and is compared in Fig. 4 with the LAR of the Lingtai section (Ding et al., 1998), another section in the eastern Loess Plateau (Fig. 1). From ~6.2 to ~5.0 Ma BP, higher eolian accumulation rate is suggested by the Lingtai section (Fig. 4) while it is not clear at Xifeng. From ~5.0 to ~3.6 Ma BP, eolian dust accumulates at a low rate, as is shown in both sections. At ~3.6 Ma, a sudden increase is observed for both sites. Another increase occurred at ~2.6 Ma BP, corresponding to the traditional boundary between the Red-Earth and the overlying loess-soil sequence.

The eolian dust from Asian drylands was not only deposited in northern China, but also in the North Pacific Ocean via transport by the northern hemisphere westerly winds (Hovan et al., 1989; Rea et al., 1998), and the fine fraction was also transported as far away as Greenland (Biscaye et al., 1997; Svensson et al., 2000). An eolian record covering the last 11.8 Ma was recovered from the North Pacific, based on the ODP cores 885/886 sites (Rea et al., 1998), and thus provides a marine record of Asian aridification. Fig. 4 shows that the variations of eolian accumulation rate recorded by the Red-Earth sections are in agreement with the eolian mass accumulation rate of the ODP

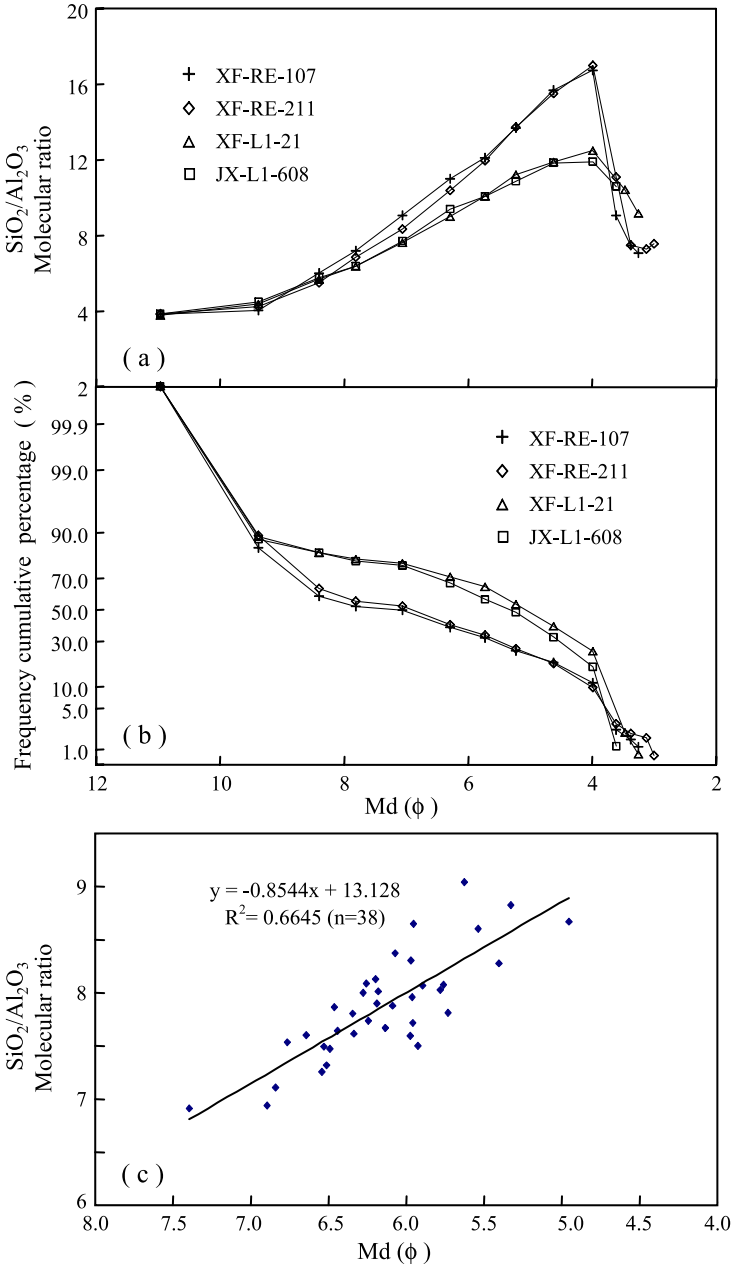

Fig. 3. Relationship between the SiO_2/Al_2O_3 molecular ratio and eolian grain size. (a) Distribution of the SiO_2/Al_2O_3 molecular ratio in different grain-size fractions for two typical loess samples and two weakly weathered Red-Earth samples. The two loess samples are from the Late Pleistocene loess L1 in the Xifeng (XF) and Jixian (JX) sections, respectively. The two Red-Earth (RE) samples are from Xifeng. (b) Cumulative percentage of the grain-size fractions of the four samples shown in a. The fractions >76 μm (Φ=3.61) represent only 2.3% in the sample XF-RE-107, 2.9% in XF-RE-211, 2.0% in XF-L1-21 and 1.15% in JX-L1-608. (c) Linear correlation between the SiO_2/Al_2O_3 molecular ratio and median grain size of 38 loess samples from Xifeng.

885/886 sites. The higher eolian accumulation rate from ~6.2 to ~5 Ma BP, as recorded at Lingtai, is also clearly documented in the North Pacific records (Rea et al., 1998). The apparent lower accumulation rate during this interval at Xifeng may be related to local depositional factors.

Thus, both marine and terrestrial proxies have documented higher dust deposition intensity from ~6.2 to ~5 Ma BP and lower intensity from ~5 to ~3.6 Ma BP. Two sharp increases in the accumulation rate are documented by all the records at ~3.6 and ~2.6 Ma BP, respectively.

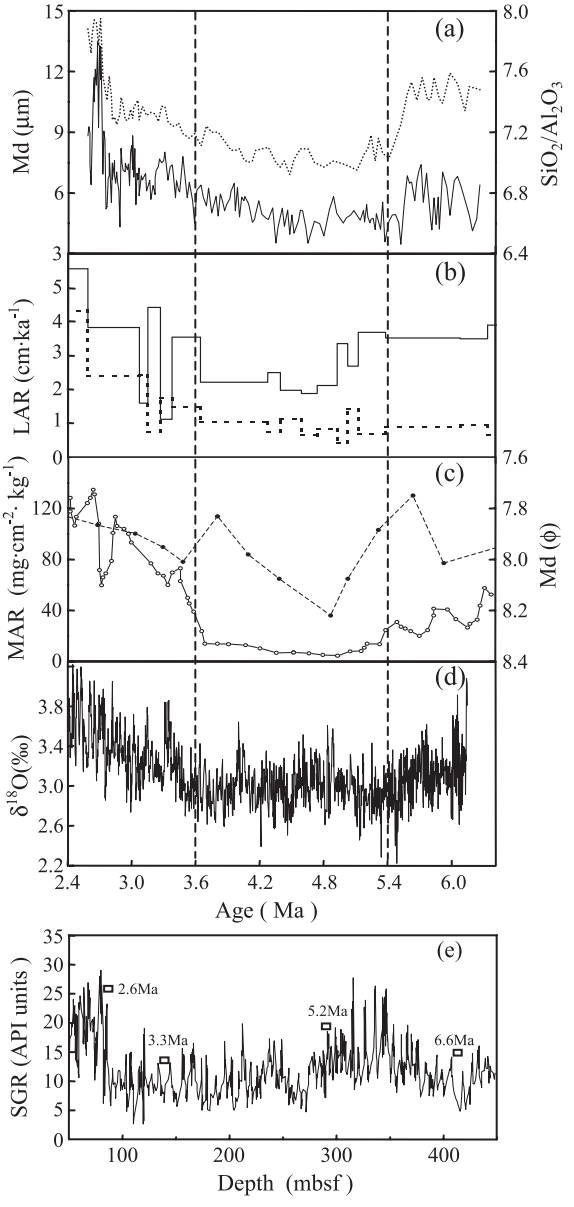

Fig. 4. Correlation of eolian grain size, accumulation rate of the Xifeng Red-Earth with the North Pacific eolian records, marine $\delta^{18}O$ record and ice-rafting terrigenous detrital sediment content in the North Pacific. (a) Variations of median grain size (solid line) and the SiO_2/Al_2O_3 molecular ratio (dashed line) versus age. The time scale was developed based on the magneto-stratigraphic results of Sun et al. (1998a) by linear interpolation. (b) Linear accumulation rates of the Xifeng (dashed line, after Sun et al., 1998a) and Lingtai (solid line, after Ding et al., 1998) Red-Earth sequences. (c) Mass accumulation rate (MAR, solid line) and eolian grain size (dotted line) from the North Pacific ODP Site 885/886 (Rea et al., 1998). (d) Marine $\delta^{18}O$ record from ODP Site 846 (Shackleton et al., 1995). (e) Natural gamma radioactivity plotted against depth with age controls. It is a measure of ice-rafted terrigenous detrital sediment content at the ODP Site 883 (DeMenocal, 1993).

1.3. Eolian grain-size changes of the Red-Earth

Because the grain size of deposited dust was affected by syn- and post-depositional weathering and pedogenesis during warm and humid periods (Guo et al., 1996, 2000), it is necessary to explore a grain-size proxy, which is able to reflect the original grain size of the deposited dust. Since the mineral assemblage in different grain-size fractions in a dust sample usually varies, which can be reflected by the chemical composition, we might expect to develop a geochemical indicator of the eolian post-depositional grain size, but prior to any subsequent weathering. For this purpose, the distribution of the most stable elements in different size fractions of the four above-mentioned samples (XF-L1-21, JX-L1-608, XF-RE-107) and XF-RE-211) was examined. The results revealed that the SiO_2/Al_2O_3 molecular ratio is closely related to grain size (Figs. 2 and 3), indicating that the chemical composition varies with grain size. For the fraction <76 μm (Φ=3.61) in each sample, the SiO_2/Al_2O_3 ratio increases with increasing grain size while the relation is reversed for the fraction >76 μm (Fig. 3a). The fact that the curves of the two Red-Earth samples are steeper than for the loess samples may be attributable to the difference in grain-size distribution between the Red-Earth and the loess. Although the ratio for the fractions >76 μm is negatively correlated with the grain size, its influence on the SiO_2/Al_2O_3 ratio of

the total sample is negligible because the cumulative weight for the fractions >76 μm represents only a proportion of less than 3% by weight of the total sample (Fig. 3b). Linear correlation between the SiO_2/Al_2O_3 ratio and the median grain size (Md) of 38 bulk loess samples from Xifeng yields a correlation coefficient (R^2) of 0.66, confirming the close relationship of the two parameters.

The SiO_2/Al_2O_3 ratio of the bulk sample can therefore be used as a suitable indicator for addressing original eolian grain-size changes. The fact that this relationship is persistent for Quaternary loess samples from Xifeng and Jixian as well as for the Tertiary Red-Earth samples suggests that it has spatial and temporal significance for the late Cenozoic eolian deposits in the Loess Plateau region. Because SiO_2 and Al_2O_3 are among the most stable elements in a wide range of climatic conditions, this index can be used on the eolian deposits in northern China. As might be expected, microscopic examination reveals that coarser fractions contain significantly more quartz, which is responsible for the higher SiO_2/Al_2O_3 ratios.

Variations of the median grain size of the Xifeng Red-Earth sequence are shown in Figs. 2 and 4, and compared with those of the SiO_2/Al_2O_3 ratio. The two proxies are coherent, confirming that post-depositional weathering processes have not significantly affected the long-term trends of eolian grain size at Xifeng.

Generally, eolian grain size is controlled most importantly by two factors: the strength of the transporting winds (Hovan et al., 1989, Rea et al., 1998; An and Porter, 1997) and the distance from the source area to the depositional site (Liu, 1985; Kukla, 1987; Ren et al., 1996; Ding et al., 1999). Since the aeolian dust deposits in northern China was transported by the Asian winter monsoon winds (Liu, 1985), the grain size must carry information on the strength of the Asian winter monsoon. The southern margin of the desert lands experienced drastic displacement during the glacial–interglacial cycles (Sun et al., 1998c). These displacements were of the order of a few hundred kilometers and must have affected the distance from the source areas for a given depositional site, which must have strongly controlled the grain-size variations in the loess sequences in China (Liu, 1985; Kukla, 1987; Ren et al., 1996), as is supported by the fact that the grain size of loess decreases from northwest to southeast in the Loess Plateau region (Liu, 1985). Recent studies along a north–south transect in the Loess Plateau confirm that eolian grain size for the same loess units is highly coherent with the distance from the desert margin (Ding et al., 1999).

In the North Pacific, the eolian mass accumulation rate is interpreted as an indication of the continental aridity while the eolian grain size mainly reflects the strength of the westerly winds (Hovan et al., 1989; Rea et al., 1998). This is because the dust deposited in the North Pacific was transported by the westerly winds, and the long distance from the source in Asia to a given site in the North Pacific, located in the East of the source region, remained relatively constant, since the changes of the desert boundaries were mainly characterized by north–south oscillations (Sun et al., 1998c). During the Quaternary, variations of the grain size of Chinese loess (e.g., Vandenberghe et al., 1997) are highly consistent with the eolian mass accumulation rates in the North Pacific (see Hovan et al., 1989), suggesting also that the former bears strong signals of the continental aridity in Asia. The similarity between the grain size of the eolian deposits in China and the mass accumulation rate in the North Pacific (Rea et al., 1998) is also observed for Late Miocene and Pliocene time (Fig. 4). In the loess-soil sequence of the last 2.6 Ma, the successful construction of the loess time scales using the grain-size parameters (An and Porter, 1997; Vandenberghe et al., 1997) indicates that eolian grain size in the Loess Plateau region has indeed coherently varied with the dust accumulation rate, suggesting that both proxies are closely linked with continental aridity.

In summary, the variations of eolian grain size for the Loess Plateau region in China resulted from the mixed effects of continental aridity in the source region (desert extent) and the strength of the dust-transporting winds. The high consistency between the eolian grain size in China and the eolian mass accumulation rate in the North Pacific, the spatial distribution pattern (Liu, 1985; Ding et al., 1999), and the coeval variations of grain size and loess accumulation rate, as demonstrated in earlier studies (An and Porter, 1997; Vandenberghe et al., 1997), suggest that extent of desert areas may have played a primary role on the grain size of Chinese loess.

1.4. Late Miocene–Pliocene aridification history of the Asian interior

The eolian dust deposited in the middle reaches of the Yellow River (Huang He) mainly originated from the desert lands in Asia, including those in northern and northwestern China (Liu, 1985). The existence of dry lands in Asia is thus one of the necessary conditions for eolian dust deposition in the Loess Plateau region. The Miocene loess-soil sequences in the western Loess Plateau indicate the onset of desertification in the Asian interior by 22 Ma ago (Guo et al., 2002). The eolian deposits younger than 6.2 Ma, as recorded in the Xifeng section, indicate that the desert lands in Asia, which were able to provide a significant amount of eolian dust, must have been constantly maintained during Late Miocene–Pliocene time. However, the finer texture and the generally lower accumulation rate of the Red-Earth compared with the overlying loess of the last 2.6 Ma suggest smaller desert extent and weaker wind strength.

Fig. 4 shows that over the whole studied period, eolian dust accumulated at a high rate from ~6.2 to ~5 Ma BP in both Loess Plateau region and North Pacific, associated with coarser eolian grain size in China. These suggest stronger continental aridity in the source regions. According to the grain-size data of the Red-Earth and the eolian mass accumulation rate in the North Pacific (Rea et al., 1998), this drier period lasted until ~5.4 Ma BP. From ~5–5.4 to ~3.6 Ma BP, eolian accumulation rates in China and in the North Pacific and eolian grain-size of the Red-Earth coherently dropped to a lower level, indicating less dry conditions in the interior of Asia. Drastic increases of eolian accumulation rate and eolian grain-size at ~3.6 Ma BP are obvious for all the records, indicating a significant strengthening of the Asian continental aridity. Another increase of the aridity occurred at ~2.6 Ma BP, as is shown by both the eolian accumulation in China and in the North Pacific, the median grain size (Md) and the SiO_2/Al_2O_3 ratio of the Red-Earth (Fig. 4).

A seasonal atmospheric circulation sufficiently energetic across the drylands is necessary to transport dust particles to the depositional site. It is generally agreed that the loess deposits were mainly brought to the Loess Plateau by the northwesterly winds, the so-called Asian winter monsoon related to a high-pressure cell over Siberia (Liu, 1985; An and Porter, 1997). The high degree of similarity between the geochemical properties of the Red-Earth and loess samples (Guo et al., 2001) suggests rather similar source areas and comparable dust-transporting trajectories. Thus, the Asian winter monsoon circulation was always the main dust-carrier during Late Miocene–Pliocene time.

Obvious discrepancies exist between the grain-size changes of the Xifeng Red-Earth (Fig. 4a) and those of the ODP Sites 885/886 (Fig. 4c). The grain-size changes in the North Pacific are interpreted as a proxy of the strength of the westerlies (Hovan et al., 1989; Rea et al., 1998). This implies again that the dominant dust-transporter for the Loess Plateau region in the Late Miocene and Pliocene was the Asian winter monsoon, rather than the westerly winds.

1.5. Links with the Tibetan uplift and the ice build-up in the northern hemisphere

Two main factors may be invoked to explain the desertification in the interior of Asia in the Late Miocene–Pliocene time. Climate models suggest that the uplift of the Tibetan Plateau may have played an important role in Asian aridification through modulating the atmospheric circulation and its barrier effect to moisture (Ruddiman and Kutzbach, 1989; Manabe and Broccoli, 1990; An et al., 2001). Another factor is the ongoing global cooling and the expansion of Arctic ice-sheet, which is likely to have had a major impact on the intensity of the winter Siberian high-pressure cell, resulting in higher continental aridity in Asia (Ruddiman and Kutzbach, 1989).

Although the timing of the Tibetan uplift is still controversial (Sun and Zheng, 1998), the available data (e.g. Li et al., 1997; Sun and Zheng, 1998) suggest that an uplift of portions of the Plateau occurred at ~3.6 Ma BP, which is synchronous with a major increase in Asian continental aridity (Fig. 4). However, the return to more humid conditions in Asia at ~5–5.4 Ma BP (Fig. 4) is difficult to explain by the Tibetan uplift because tectonic impact on climate should be a unidirectional step during this interval. Another strengthening of the Asian aridification occurred at ~2.6 Ma BP although no evidence indicates a major uplift of the Tibetan Plateau

at that time. These suggest that other factors have also played a major role on the development of Asian desertification.

The marine $\delta^{18}O$ records of benthic foraminifers are commonly accepted as an indication of global cooling and ice-volume variations, which include both the signals from the southern and northern hemispheres (Shackleton and Pisias, 1985; Shackleton et al., 1990, 1995). The amount of ice-rafted debris in the circum-Arctic region can also be regarded as a good indicator of the development of the circum-Arctic sea-ice and ice-sheets (DeMenocal, 1993).

In Fig. 4, the Late Miocene–Pliocene Asian aridification history, as indicated by the Xifeng eolian accumulation rate and grain-size proxies, is compared with the ODP 846 $\delta^{18}O$ record (Fig. 4d) (Shackleton et al., 1995), an indication of global ice-volume variations, and with natural gamma radioactivity (Fig. 4e), a measure of ice-rafted, terrigenous, detrital sediment content at the ODP Site 883 in the North Pacific (DeMenocal, 1993). The former includes both the signals from the southern and northern hemispheres (Shackleton et al., 1995) while the amount of ice-rafted debris may reflect the development of the ice-sheets in the northern hemisphere (DeMenocal, 1993). Although ice-rafting history near the Arctic region may be traced back to ~ 12 Ma BP, a real ice-sheet in the Arctic region appeared at ~6–7 Ma BP in Greenland (Jansen and Sjoholm, 1991). Fig. 4 shows that the high Asian continental aridity from ~6.2 to ~5 Ma BP is correlative with intense ice-rafting events in the Arctic region, and with a cooler events indicated by the marine $\delta^{18}O$ record. The lower aridity from ~5.0 to ~3.6 Ma BP correlates with the lower intensity of ice-rafting events and warmer conditions. The strong aridification at ~2.6 Ma BP, indicated by the intense eolian deposition (the lower boundary of the loess-soil sequence) in northern China is synchronous with a sudden increase in the amount of ice-rafted debris. Although the increase in aridity at ~3.6 Ma BP has no equally clear counterpart in the ODP 883 ice-rafting record, all of the marine $\delta^{18}O$ records (e.g. Shackleton et al., 1995) indicate a similar increase in global ice-volume at that time.

The aridification history in the Late Miocene and Pliocene in East Asia is therefore highly consistent with the ongoing cooling and the development of the

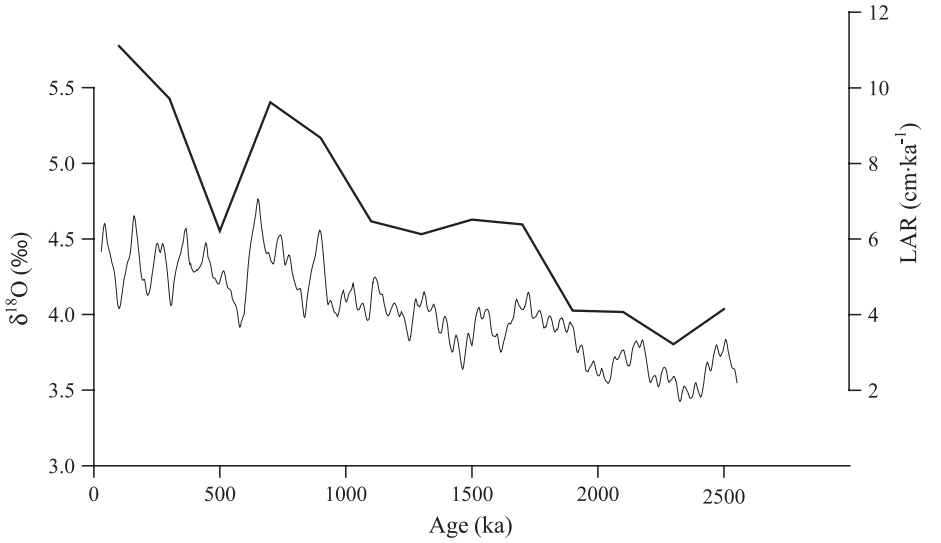

Fig. 5. Coupled changes between the loess accumulation rate in the central Loess Plateau (Xifeng, thick line) and the marine $\delta^{18}O$ record (fine line). Calculation of the loess accumulation rate of the Xifeng loess-soil sequence was made at 200-ka intervals. The time scale is from Kukla and An (1989) and revised by the new geomagnetic polarity time scale (Cande and Kent, 1995). The composite marine $\delta^{18}O$ sequence shown here is a 20-point moving average curve based on the data from V19-30 (Shackleton and Pisias, 1985), ODP 677 (Shackleton et al., 1990) and ODP 846 sites (Shackleton et al., 1995).

Arctic ice-sheet. The stepwise increases of loess accumulation rate at ~1.8 and ~0.9 Ma BP as recorded by the loess of the last 2.6 Ma also strongly support this interpretation (Fig. 5). This suggests that the development of the northern hemispheric ice-sheets had played an important role in driving the Asian aridification over the past 6 Ma. The ~0.9 Ma age boundary would also be consistent consistent with another uplift phase of the Himalayas–Tibetan complexes (Amano and Taira, 1992; Sun and Zheng, 1998; Lu et al., 2001).

The links between the Asian aridification and northern hemisphere cooling are likely to be explainable by two mechanisms. First, ocean cooling would provide less moisture to the continents, and thus lead to drier conditions in Asia. Second, cooler high-latitudes, extended sea-ice and ice-sheets in the arctic region strengthened the Siberian high-pressure cell, which in turn, significantly intensify the continental aridity in the interior of Asia (Ruddiman and Kutzbach, 1989).

Our results therefore indicate that both the Tibetan uplift and the ongoing global cooling/arctic ice-building processes have played major role on the aridification in the interior of Asia during the in the late Cenozoic. Their roles are not mutually exclusive.

2. Conclusions

Until now, most of the Late Miocene and Pliocene climatic information about the East Asian drylands has been recovered from marine records (e.g. Rea et al., 1998). The Xifeng Red-Earth Formation, however, provides a continuous terrestrial record, having documented a detailed history of the East Asian continent for this period. This terrestrial record is largely consistent with the marine records from the North Pacific (Rea et al., 1998).

The Asian desertification was started by 22 Ma ago (Guo et al., 2002). Since the existence of arid lands in East Asia is a necessary condition for eolian dust deposition in northern China, the eolian origin of a major part of the Red-Earth indicates that sizeable desert lands in East Asia must have been maintained during Late Miocene–Pliocene time, and were able to provide a significant amount of eolian dust. The continental aridity was stronger from ~6.2 to ~5 Ma BP, weaker from ~5 to ~3.6 Ma and then strengthened at ~3.6, and more significantly at ~2.6 Ma BP. The most important aridification event at ~3.6 Ma BP corresponds to an uplift of portions of the Tibetan Plateau. The detailed changes are, however, in good agreement with the ongoing global cooling and the Arctic ice-sheet development as reflected by the record of ice-drafted terrigenous materials and marine $\delta^{18}O$ record. Our results therefore suggest that both the Tibetan uplift and the ongoing global cooling/arctic ice-building processes have played major role on the aridification in the interior of Asia during Late Miocene and Pliocene time, and that their roles are not mutually exclusive.

Acknowledgements

This work was supported by the National Natural Science Foundation of China (Projects 40231001 and 40024202), the Chinese Academy of Sciences (KZCX-118 and KZCX2-SW-113). Participation of PEB was supported by the U.S. National Science Foundation under Grant No. OPP96-25287. This is also a LDEO Contribution No. 6238.

References

Amano, K., Taira, A., 1992. Two phase uplift of high Himalaya since 17 Ma. Geology 20, 391–394.

An, Z.S., Porter, S.C., 1997. Millennial-scale climatic oscillations during the last interglaciation in central China. Geology 25, 603–606.

An, Z.S., Kutzbach, J.E., Prell, W.L., Porter, S.C., 2001. Evolution of Asian monsoons and phased uplift of the Himalaya–Tibetan Plateau since Late Miocene time. Nature 411, 62–66.

Biscaye, P.E., Grousset, F.E., Revel, M., Van der Gaast, S., Zielinski, G.A., Vaars, A., 1997. Asian provenance of last glacial maximum dust in the GISP2 ice core, summit, Greenland. Journal of Geophysical Research 102, 26765–26781.

Cande, S.C., Kent, D.V., 1995. Revised calibration of the geomagnetic polarity timescale for the late Cretaceous and Cenozoic. Journal of Geophysical Research 100, 6093.

DeMenocal, P., 1993. Wireline logging of the North Pacific transect. JOIDES Journal 19, 29.

Ding, Z.L., Sun, J.M., Yang, S.L., Liu, T.S., 1998. Preliminary magnetostratigraphy of a thick eolian red clay-loess sequence at Lingtai, the Chinese Loess Plateau. Geophysical Research Letters 25, 1225–1228.

Ding, Z.L., Sun, J.M., Rutter, N.W., Rokosh, D., Liu, T.S., 1999. Changes in sand content of loess deposits along a north–south transect of the Chinese Loess Plateau and the implication for desert variations. Quaternary Research 52, 56–62.

Guo, Z.T., Fedoroff, N., An, Z.S., 1991. Genetic types of the Holocene soil and the Pleistocene palaeosols in the Xifeng loess section in central China. In: Liu, T.S., Ding, Z.L., Guo, Z.T. (Eds.), Loess, Environment and Global Change. Science Press, Beijing, pp. 93–111.

Guo, Z.T., Liu, T.S., Guiot, J., Wu, N.Q., Lu, H.Y., Han, J.M., Liu, J.Q., Gu, Z.Y., 1996. High frequency pulses of east Asian monsoon climate in the last two glaciations: link with the North Atlantic. Climate Dynamics 12, 701–709.

Guo, Z.T., Liu, T.S., Fedoroff, N., Wei, L.Y., Ding, Z.L., Wu, N.Q., Lu, H.Y., Jiang, W.Y., An, Z.S., 1998. Climate extremes in loess of China coupled with the strength of deep-water formation in the North Atlantic. Global and Planetary Change 18, 113–128.

Guo, Z.T., Biscaye, P., Wei, L.Y., Chen, X.F., Peng, S.Z., Liu, T.S., 2000. Summer monsoon variations over the last 1.2 Ma from the weathering of loess-soil sequences in China. Geophysical Research Letters 27, 1751–1754.

Guo, Z.T., Peng, S.Z., Hao, Q.Z., Biscaye, P.E., Liu, T.S., 2001. Origin of the Miocene–Pliocene Red-Earth Formation at Xifeng in northern China and implications for paleoenvironments. Palaeogeography, Palaeoclimatology, Palaeoecology 170, 11–26.

Guo, Z.T., Ruddiman, W.F., Hao, Q.Z., Wu, H.B., Qiao, Y.S., Zhu, R.X., Peng, S.Z., Wei, J.J., Yuan, B.Y., Liu, T.S., 2002. Onset of Asian desertification by 22 Myr ago inferred from loess deposits in China. Nature 416, 159–163.

Hovan, S.A., Rea, D.K., Pisias, N.G., Shackleton, N.J., 1989. A direct link between the China loess and marine $\delta^{18}O$ records: aeolian flux to the north Pacific. Nature 340, 296–298.

Jansen, E., Sjoholm, J., 1991. Reconstruction of glaciation over the past 6 Myr from ice-borne deposits in the Norwegian Sea. Nature 349, 600–603.

Kukla, G., 1987. Loess stratigraphy in central China. Quaternary Science Reviews 6, 191–219.

Kukla, G.J., An, Z.S., 1989. Loess stratigraphy in central China. Palaeogeography, Palaeoclimatology, Palaeoecology 72, 203–225.

Li, J.J., Fang, X.M., Van der Voo, R., Zhu, J.J., Mac Niocaill, C., Cao, J.X., Zhong, W., Chen, H.L., Wang, J.M., Zhang, Y.C., 1997. Late Cenozoic magnetostratigraphy (11–0 Ma) of the Dongshanding and Wangjiashan sections in the Longzhong Basin, western China. Geologie en Mijnbouw 76, 121–134.

Liu, T.S., 1985. Loess and the Environment. China Ocean Press, Beijing. 251 pp.

Lu, H.Y., Wang, S.M., Wu, N.Q., Tong, G.B., Yang, X.D., Shen, C.M., Li, S.J., Zhu, L.P., Wang, L., 2001. A new pollen record of the last 2.8 Ma from the Co Ngoin, central Tibetan Plateau. Science in China. Series D 44, 292–300 (Suppl.).

Manabe, S., Broccoli, A.J., 1990. Mountains and arid climate of middle latitudes. Science 247, 192–195.

Qiang, X.K., Li, Z.X., Powell, C.McA., Zheng, H.B., 2001. Magnetostratigraphic record of the Late Miocene onset of the East Asian monsoon, and Pliocene uplift of northern Tibet. Earth and Planetary Science Letters 187, 83–93.

Rea, D.K., Snoeckx, H., Joseph, L.H., 1998. Late Cenozoic eolian deposition in the North Pacific: Asian drying, Tibetan uplift, and cooling of the northern hemisphere. Paleoceanography 13, 215–224.

Ren, J.Z., Ding, Z.L., Liu, T.S., Sun, J.M., Zhou, X.Q., 1996. Climatic changes on millennial time scales: evidence from a high-resolution loess record. Science in China. Series D 39, 449–459.

Ruddiman, W.F., Kutzbach, J.E., 1989. Forcing of late Cenozoic northern hemisphere climate by plateau uplift in southern Asia and the American West. Journal of Geophysical Research 94, 18409–18427.

Shackleton, N.J., Pisias, N.G., 1985. Atmospheric carbon dioxide, orbital forcing, and climate. In: Sundquist, E.T., Broeker, W.S. (Eds.), The Carbon Cycle and Atmospheric CO2: Natural Variations Archean to Present. Geophysical Monograph, vol. 32, pp. 412–417.

Shackleton, N.J., Berger, A., Peltier, W.R., 1990. An alternative astronomical calibration of the lower Pleistocene timescale based on ODP Site 677. Transactions of the Royal Society of Edinburgh. Earth sciences 81, 251–261.

Shackleton, N.J., Hall, M.A., Pate, D., 1995. Pliocene stable isotope stratigraphy of Site 846. Proceedings of the Ocean Drilling Program. Scientific results 138, 337–355.

Sun, H.L., Zheng, D., 1998. Formation, Evolution and Development of Qinghai-Xizang (Tibetan) Plateau. Guangdong Science and Technology Press, Guangzhou, China. 350 pp.

Sun, D.H., An, Z.S., Shaw, J., Bloemendal, J., Sun, Y.B., 1998a. Magnetostratigraphy and paleoclimatic significance of late Tertiary Aeolian sequence in the Chinese Loess Plateau. Geophysical Journal International 134, 207–212.

Sun, D.H., Shaw, J., An, Z.S., Chen, M.Y., Yue, L.P., 1998b. Magnetostratigraphy and paleoclimatic interpretation of a continuous Late Cenozoic eolian sediments from the Chinese Loess Plateau. Geophysical Research Letters 25, 85–88.

Sun, J.M., Ding, Z.L., Liu, T.S., 1998. Desert distributions during the glacial maximum and climate optimum: example of China. Episode 21, 28–31.

Svensson, A., Biscaye, P.E., Grousset, F.E., 2000. Characterization of late glacial continental dust in the Greenland GRIP ice core. Journal of Geophysical Research 105, 4637–4656.

Vandenberghe, J., An, Z.S., Nugteren, G., Lu, H.Y., Huissteden, K.V., 1997. New absolute time scale for the Quaternary climate in the Chinese loess region by grain-size analysis. Geology 25, 35–38.

Yue, L.P., 1995. Palaeomagnetic polarity boundaries recorded in Chinese loess and red clay, and geological significance. Acta Geophysica Sinica 38, 311–319 (in Chinese with English abstract).

Zheng, H.B., An, Z.S., Shaw, J., 1992. New contributions to Chinese Plio-Pleistocene magnetostratigraphy. Physics of the Earth and Planetary Interiors 70, 146–153.